ISSN 1063-780X, Plasma Physics Reports, 2022, Vol. 48, No. 11, pp. 1137–1141. © Pleiades Publishing, Ltd., 2022.
Russian Text © The Author(s), 2022, published in Fizika Plazmy, 2022, Vol. 48, No. 11, pp. 1005–1009.

MAGNETIC TRAPS

Studies of Trapping and Accumulation of Fast Ions in Preliminary Experiments on Neutral Beam Injection at the GOL-NB Facility

V. V. Postupaev[a], *, V. I. Batkin[a], A. V. Burdakov[a], V. S. Burmasov[a], I. A. Ivanov[a], K. N. Kuklin[a], Yu. A. Lykova[a], K. I. Mekler[a], N. A. Mel'nikov[a], A. V. Nikishin[a], S. V. Polosatkin[a], A. F. Rovenskikh[a], E. N. Sidorov[a], V. F. Sklyarov[a], and D. I. Skovorodin[a]

[a] *Budker Institute of Nuclear Physics of the Siberian Branch of the Russian Academy of Sciences, Novosibirsk, 630090 Russia*

**e-mail: V.V.Postupaev@inp.nsk.su*

Received April 20, 2022; revised May 25, 2022; accepted June 15, 2022

Abstract—The results are presented from preliminary experiments on neutral beam injection with the power of approximately 1 MW into the central trap of the GOL-NB facility. The main technical task of the work was the integrated commissioning of all systems and basic diagnostics. The results are presented on the attenuation of neutral beams in plasma and the parameters of the fast ion population. In the regimes under discussion, the attenuation factor of the flow of injected particles of heating beams reaches 40% at the simultaneous start of the initial plasma accumulation in the trap and its heating by neutral beams. The dynamics of accumulation and energy spectrum of the fast ion population formed in plasma as a result of neutral beam injection are discussed, and the physical mechanisms are analyzed that can provide for the observed spectrum of fast ions.

Keywords: plasma, open magnetic trap, multiple-mirror trap, GOL-NB, neutral injection, fast ions, plasma diagnostics

DOI: 10.1134/S1063780X22600682

1. INTRODUCTION

The multiple-mirror magnetic systems were proposed in [1, 2] as a way to increase the plasma lifetime in open traps. In such systems, the magnetic field is corrugated (periodically modulated along the facility axis). As the plasma expands along the magnetic field, in each elementary cell of the multiple-mirror system, the interaction of populations of transient and locally trapped plasma particles results in the appearance of the friction force, which slows down the plasma flow escaping along the facility axis. This confinement method is most efficient at moderate collisionalities $\nu^* = l/\lambda \approx 1$, where l is the period of the magnetic field corrugation (distance between maxima), and λ is the mean free path of ions [3]. The results of studies in this field of research are presented in more detail in [4]. In the existing configuration, the primary task of the GOL-NB facility should be the studies the operating regime with $\nu^* \approx 1$ and direct demonstration the efficiency of plasma confinement in the facility sections with the multiple-mirror magnetic field [5, 6]. In the future, after installing the additional plasma heating systems, the transition could be possible to the regime with $\nu^* \ll 1$, which is more interesting from the point of view of fusion applications [7].

The experiments in the GOL-NB design configuration started at the beginning of 2021. Before the beginning of this work, the problems were solved of transporting the low-temperature starting plasma with $\nu^* \gg 1$ through the section with the multiple-mirror magnetic field [8] and filling the central trap with the starting plasma with the density of $n(0) \approx 10^{20}$ m^{-3} at the facility axis and the electron temperature of $T \approx$ 5 eV [9]. In this work, we report the results from preliminary experiments on the injection of two hydrogen neutral beams with the total power of approximately 1 MW into the GOL-NB central trap. The main task was the integrated commissioning of all systems and basic plasma diagnostics. The results are presented on the attenuation of neutral beams in plasma and the parameters of the fast ion population forming in plasma.

2. EXPERIMENTAL DEVICE AND DIAGNOSTICS

The GOL-NB facility consists of the central trap of the gasdynamic type with the length of 2.5 m and the magnetic induction of $B = 0.3$ T at the center, the 3-m-long sections of the high magnetic field ($B = 4.5$ T) attached to it, and the end magnetic flux expanders. Inside the expanders, there are plasma receiving endplates and plasma gun with the arc source of hydrogen plasma [10]. The high-magnetic-field sections can be used in the solenoidal configuration with the uniform magnetic field or in the multiple-mirror configuration with the depth of the magnetic field corrugation $R_m = B_{max}/B_{min} = 1.4$ and the corrugation period of 22 cm. The facility design is described in more detail in [9]. In the experiments discussed here, the high-magnetic-field sections were used in the solenoidal configuration with $B = 2.25$ T. Two beams of hydrogen atoms [11] with the energy of $E = 25$ keV and the total power of up to 1.1 MW are injected into the plasma normally to the axis at the points $z = \pm 0.4$ m (the longitudinal coordinate z is counted from the midplane of the trap). The feature of the experimental scenario was that the plasma gun and heating neutral beams were switched on almost simultaneously (see Fig. 1). This is not optimal from the point of view of the efficiency of trapping fast particles by plasma, but this makes it possible to use neutral beams as diagnostics during the entire plasma discharge.

Previously, in [8, 9], we used four-electrode Langmuir probes [12] for measuring the parameters of the start plasma. Since the presence of probes in the central trap is incompatible with the injection of neutral beams, the probe measurements were performed in the high-field section at $z = 1.26$ m. The attenuation of neutral beams by the plasma served as the diagnostics of plasma density dynamics in the trap. The radial beam profile was measured using the multiwire detector, which can record either the secondary emission currents or changes in the resistivity of wires during their heating by the passed beam. The second method is insensitive to the magnetic field and particle charge, but has low time resolution. The results obtained using both methods are consistent.

The density dynamics of plasma and population of fast ions formed as a result of neutral beam injection into the plasma was studied using optical spectral diagnostics, which measured plasma emission in the vicinity of the H_α line of hydrogen atom [13]. This diagnostics includes the MDR-12 spectrometer with the SDU-285 digital camera that measured plasma spectra with time resolution of 10 μs, the MDR-23 spectrometer with the array of FEU-83 photomultipliers tuned for measuring certain spectral intervals, and the SDU-285 camera with the narrow-band interference filter, which recorded the spatial distribution of radiation. Spectral instruments record plasma emission at an angle of 45° to the direction of the neutral beam injection at $z = \pm 0.4$ m. This makes it possible to distinguish between the plasma emission and the radiation emitted by the population of fast ions due to the Doppler shift of the lines.

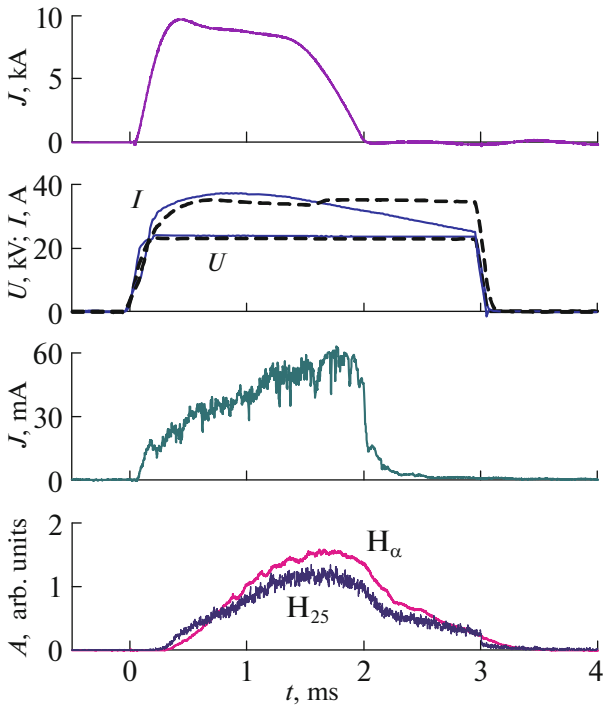

Fig. 1. Basic signals in the NB5941 experiment from top to bottom: discharge current in plasma gun; accelerating voltages U and currents I in high-voltage circuits of two neutral beam injectors (differ in types of lines); saturation ion current of Langmuir probe installed at $r = 0$, $z = 1.26$ m; and signals of photomultipliers tuned to H_α line corresponding to cold plasma and Doppler-shifted H_α line corresponding to 25-keV-ions (these traces are denoted as H_α and H_{25}, respectively).

The spectrum of fast particles was measured using the neutral particle analyzer, which was also located at $z = -0.4$ m. The design of the analyzer is similar to the designs of similar devices previously manufactured for the C-2 and MST facilities [14]. The detecting system of the analyzer included 11 channels detecting particles with energies from 6 to 25 keV with the energy resolution of approximately 4 keV. The analyzer detected particles escaping from the plasma normally to the axis. The aiming point was shifted from the axis by the Larmor radius of fast ion $r = 5$ cm.

3. EXPERIMENTAL RESULTS

In this section, we will discuss the results of the specific experiment NB5941. The signals characterizing the plasma dynamics in the facility are shown in Fig. 1. The discharge current lasts for approximately 2 ms; the neutral beam injection duration is set to

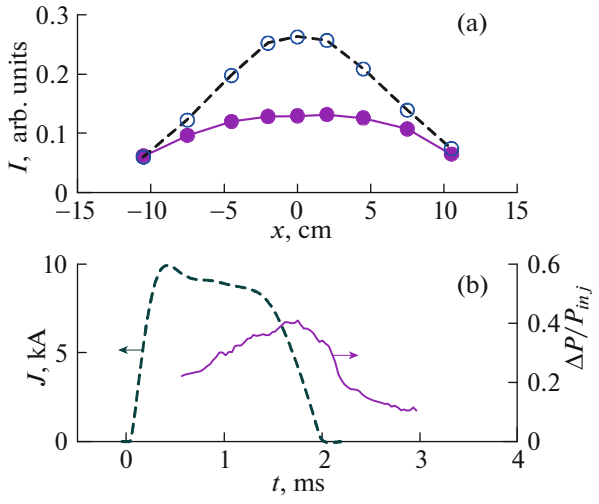

Fig. 2. Top: neutral beam profiles obtained from signals of multiwire detector operating in the mode of secondary emission measurements during time interval t = [1.35–1.85] ms; open and solid circles correspond to experiments NB5941 (with plasma) and NB5939 (without plasma), respectively; and x is transverse coordinate. Bottom: dynamics of discharge current of plasma gun (dashed line) and attenuation of heating beam in plasma (solid line) in experiment NB5941.

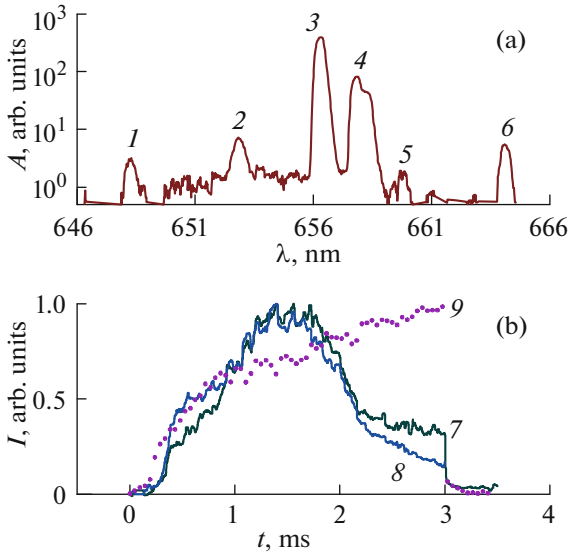

Fig. 3. Plasma emission spectrum in the vicinity of H_α line (656.28 nm) in cross section of injection of fast hydrogen neutral beam for time interval t = [1.5–1.7] ms. Observations are performed at an angle of 45° to direction of beam propagation. (*1*) NII line (648.2 nm); (*2*) H_α line of beam atoms with energies of 25 keV; (*3*) H_α line of target plasma; (*4*) CII lines (657.8 and 658.3 nm); (*5*) H_α line of beam atoms emission reflected from the opposite chamber wall; (*6*) OII line (664.1 nm); (*7*) dynamics of accumulated fast protons; (*8*) electron density dynamics; and (*9*) current density of fast atoms.

3 ms, in order to observe the plasma also in the course of its decay. The plasma density in the output high-field section increases during the gun operation that indicates the accumulation of plasma in the trap. There is a jump on the signal of the spectral channel corresponding to the beam atoms with energy of 25 keV at time of switching off the injection.

The radial profiles characterizing the beam attenuation in the plasma are shown in Fig. 2. By the end of the plasma gun operation, the attenuation factor integrated over the beam cross section reaches 40%. We note that the plasma "shadow" does not accurately correspond to the plasma geometrical parameters, since the beams are focused at a distance of 0.5 m before the trap axis. In this operating regime, the initial plasma diameter is less than the diameter of the heating neutral beam that reduces the integrated trapping efficiency.

The emission spectrum in the spectral band near the H_α line is shown in Fig. 3. The emission of cold atoms in the wavelength range near 656.28 nm is the most intense (*3* in Fig. 3); it can be associated with the target plasma. The spectrum contains the H_α line emitted by the injected atoms, which is Doppler-shifted to the blue side (*2*). Their emission, reflected from the opposite vacuum chamber wall, falls into the red side (*5*). The spectrum also contains lines of impurity ions. The radiation corresponding to the wings of the H_α line is emitted by the atoms produced during the charge exchange process of fast ions in the plasma. The spectrum dynamics can be used to qualitatively estimate the densities of electrons n_e and fast protons n_{fp} (assuming the spatially uniform source):

$$n_e \propto \frac{I_b}{J_b}, \quad n_{fp} \propto \frac{I_f}{I_s} \times \frac{I_b}{J_b},$$

where I_b is the H_α line intensity of the beam atoms, J_b is the known current density of the injected atoms, I_f is the H_α line intensity of the fast atoms produced during charge exchange of fast ions, and I_s is the H_α line intensity of the target plasma. The results are given in Fig. 3 in the bottom.

The signals of two analyzer channels and the energy spectrum of charge exchange neutrals are shown in Fig. 4. The ions with energies close to the injection energy dominate in the spectrum, which indicates the presence of additional channel of fast ions loss. A possible loss channel is the charge exchange in collisions with the background gas in the plasma. The measured spectrum was compared with the predictions of the simple model of dynamics of fast ion distribution function, which takes into account the drag on electrons and loss of particles due to the charge exchange in collisions with molecular hydrogen. In the quasi-stationary case, the distribution function of ions over

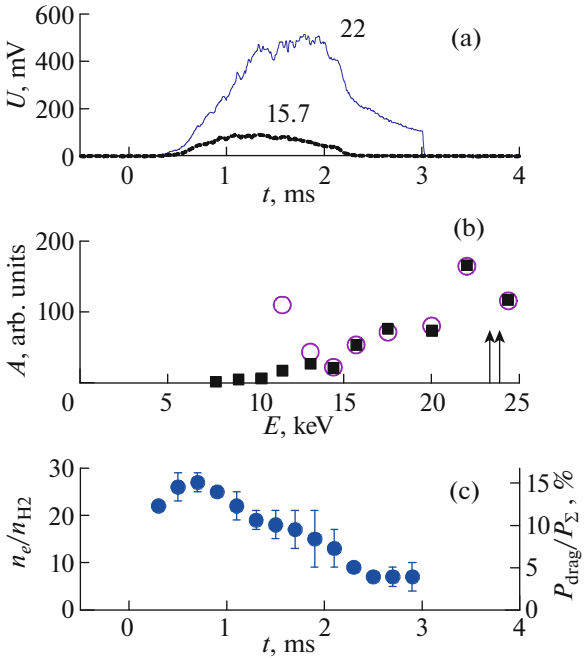

Fig. 4. (a) Flux dynamics of charge exchange neutrals in 22- and 15.7-keV channels; (b) energy spectrum measured at $t = 0.7$ ms (circles) and its fit by model spectrum (squares); and (c) ratio $\chi = n_e/n_{H2}$ of mean densities of electrons and neutral gas (averaged along ion trajectory) calculated for $T = 5$ eV. Arrows correspond to energies of neutral beams.

the total velocity $f_i(v_i)$ can be obtained by integrating the following kinetic equation:

$$\frac{\partial}{\partial v_i}\left(-f_i\frac{v_i}{\tau_{drag}(v_i)}\right) = -\frac{f_i}{\tau_{cx}(v_i)},$$

whence

$$f_i(v_i) \sim \frac{\tau_{drag}}{v_i}\exp\int_{v_i}^{v_{inj}}\frac{\tau_{drag}(v_i')}{\tau_{cx}(v_i')}\frac{dv_i'}{v_i'},$$

where v_{inj} is the ion velocity at the injection energy, while τ_{drag} and τ_{cx} are the characteristic times of deceleration and loss of fast ions due to charge exchange.

In turn, these characteristic times can be expressed as follows [15]:

$$\tau_{cx} = \left(n_{H2}\sigma_{cx}v_i\right)^{-1},$$

$$\tau_{drag} = \left(n_e\sigma_{ie}v_i\int_0^{\frac{m_e v_i^2}{2}} f_M(T_e, E_e)dE_e\right)^{-1},$$

where f_M is the Maxwell distribution function, $\sigma_{ie} = 4\pi a_B^2\Lambda\frac{m_i}{m_e}\left(\frac{Ry}{E_i}\right)^2$ is the transport cross section for collisions of fast ions with electrons, σ_{cx} is the charge exchange cross section, Λ is the Coulomb logarithm, $R_y = 13.6$ eV is the Rydberg constant, and a_B is the Bohr radius.

Thus, at a given electron temperature, the shape of the distribution function is determined by one parameter $\chi = n_e/n_{H2}$, the ratio of the averaged (along the ion trajectory) electron and gas densities. The result of fitting the model distribution function to the measured spectrum of fast particles is also shown in Fig. 4. The distribution function was calculated using data of the six highest-energy analyzer channels with allowance for their different spectral sensitivity (in low-energy channels, the contribution appears of particles with half the energy from that of the accelerated hydrogen molecules; so, these channels were not taken into account).

The dynamics of the ratio of average densities of electrons and background gas in plasma is shown in Fig. 4c. Integration of the obtained distribution function of fast ions provides the fraction of power transported from the trapped ions to plasma electrons. The maximum fraction is approximately 15% of the trapped beam power (see Fig. 4c, right axis). We note that latter value is almost independent of the assumed electron temperature and is more accurate than the χ parameter.

4. DISCUSSION AND CONCLUSIONS

The GOL-NB physical project [5, 6] suggests that at densities $n > 3 \times 10^{19}$ m^{-3}, the energy of neutral beams should be quickly thermalized in plasma due to deceleration in collisions with electrons. In this case, the density of fast ions population will be low, and the system will be safe in terms of development of the main fast ion instabilities. The plasma temperature is set as a result of reaching the energy balance between the neutral beam heating and longitudinal gas-dynamic losses. In this case, according to calculations [16], the regime with $\nu^* \approx 1$ favorable for multiple-mirror plasma confinement will be established in the GOL-NB facility.

In the experiments presented, the target plasma diameter was less than the design diameter. This resulted in two consequences. First, a part of the neutral beam passed through the low-density peripheral plasma, thereby reducing the average trapping coefficient. Second, the Larmor radius of fast ions (approximately 65 mm) exceeded the plasma column radius (approximately 40 mm); therefore, the considerable sections of their trajectories passed through the low-dense peripheral plasma. Thus, the charge-exchange losses of fast ions became more important.

The low-temperature start plasma was created by the plasma gun. In this case, the densest central part of the plasma is stabilized due to the line-tying of the magnetic field to the vacuum chamber end within the limits of the magnetic surface, which starts from the aperture in the plasma collector, through which the start plasma is injected along the magnetic field [9]. During the plasma accumulation in the central trap, plasma halo gradually forms within the magnetic surface bounded by the limiters. It is assumed that this peripheral part of plasma will be stabilized using the vortex confinement technique, similar to how it is performed at the GDT facility [17]. In the experiments performed, a gradual increase was observed in the density of particles confined in the halo region. Therefore, when increasing the duration of plasma gun operation and optimizing the plasma generation regime with the increased magnetic field near the gun, it becomes possible to simultaneously improve the efficiency of neutral beams trapping in the plasma target and decrease the share of charge exchange losses.

The main result of the series of experiments conducted is the demonstration of full operabilities of the facility and available diagnostics in the design configuration of GOL-NB. Based on the results of control experiments on neutral beam injection into residual gas, it can be stated that there are no considerable losses of fast ions due to deviations of the magnetic field from the design value. In this stage of studies, in order to increase the target plasma density in the trap, the magnetic field in the high-field sections was set to be $B = 2.25$ T. Experiments with $B = 4.5$ T were also performed. In this case, the neutral beam trapping efficiency was expectedly lower, but an increase in the mirror ratio from $R = 7.5$ to $R = 15$ reduces the gasdynamic longitudinal losses by a factor of two.

FUNDING

The assembly and operations of the GOL-NB facility was supported by the Ministry of Science and Higher Education of the Russian Federation. The studies of plasma stability in the GOL-NB facility were supported by the Russian Science Foundation (project no. 21-12-00133); https://rscf.ru/en/project/21-12-00133/.

REFERENCES

1. G. I. Budker, V. V. Mirnov, and D. D. Ryutov, JETP Lett. **14**, 212 (1971).
2. B. G. Logan, A. J. Lichtenberg, M. A. Lieberman, and A. Makhijani, Phys. Rev. Lett. **28**, 144 (1972). https://doi.org/10.1103/PhysRevLett.28.144
3. V. V. Mirnov and D. D. Ryutov, Nucl. Fusion **12**, 627 (1972). https://doi.org/10.1088/0029-5515/12/6/001
4. A. V. Burdakov and V. V. Postupaev, Phys.–Usp. **61**, 582 (2018). https://doi.org/10.3367/UFNe.2018.03.038342
5. V. V. Postupaev, A. V. Burdakov, and A. A. Ivanov, Fusion Sci. Technol. **68**, 92 (2015). https://doi.org/10.13182/FST14-846
6. V. V. Postupaev, V. I. Batkin, A. D. Beklemishev, A. V. Burdakov, V. S. Burmasov, I. S. Chernoshtanov, A. I. Gorbovsky, I. A. Ivanov, K. N. Kuklin, K. I. Mekler, A. F. Rovenskikh, E. N. Sidorov, and D. V. Yurov, Nucl. Fusion **57**, 036012 (2017). https://doi.org/10.1088/1741-4326/57/3/036012
7. P. A. Bagryansky, A. D. Beklemishev, and V. V. Postupaev, J. Fusion Energy **38**, 162 (2019). https://doi.org/10.1007/s10894-018-0174-1
8. V. V. Postupaev, V. I. Batkin, A. V. Burdakov, V. S. Burmasov, I. A. Ivanov, K. N. Kuklin, K. I. Mekler, A. F. Rovenskikh, and E. N. Sidorov, Plasma Phys. Control. Fusion **62**, 025008 (2020). https://doi.org/10.1088/1361-6587/ab53c2
9. V. V. Postupaev, V. I. Batkin, A. V. Burdakov, V. S. Burmasov, I. A. Ivanov, K. N. Kuklin, Yu. A. Lykova, N. A. Melnikov, K. I. Mekler, A. V. Nikishin, S. V. Polosatkin, A. F. Rovenskikh, E. N. Sidorov, and D. I. Skovorodin, Nucl. Fusion **62**, 086003 (2022). https://doi.org/10.1088/1741-4326/ac69fa
10. I. A. Ivanov, V. I. Batkin, A. V. Burdakov, K. N. Kuklin, K. I. Mekler, V. V. Postupaev, A. F. Rovenskikh, and E. N. Sidorov, Plasma Phys. Rep. **47**, 938 (2021). https://doi.org/10.1134/S1063780X21090026
11. V. I. Batkin, E. E. Bambutsa, A. V. Burdakov, V. S. Burmasov, M. R. Gafarov, and R. V. Voskoboinikov, AIP Conf. Proc. **1771**, 030010 (2016). https://doi.org/10.1063/1.4964166
12. E. N. Sidorov, V. I. Batkin, A. V. Burdakov, I. A. Ivanov, K. N. Kuklin, K. I. Mekler, A. V. Nikishin, V. V. Postupaev, and A. F. Rovenskikh, J. Instrum. **16**, T11006 (2021). https://doi.org/10.1088/1748-0221/16/11/T11006
13. A. V. Nikishin, I. A. Ivanov, V. I. Batkin, A. V. Burdakov, K. N. Kuklin, K. I. Mekler, V. V. Postupaev, and A. F. Rovenskikh, Plasma Phys. Rep. **48**, 220 (2022). https://doi.org/10.1134/S1063780X22030114
14. S. Polosatkin, V. Belykh, V. Davydenko, R. Clary, G. Fiksel, A. Ivanov, V. Kapitonov, D. Liu, V. Mishagin, M. Tiunov, and R. Voskoboynikov, Nucl. Instrum. Methods Phys. Res., Sect. A **720**, 42 (2013). https://doi.org/10.1016/j.nima.2012.12.039
15. B. A. Trubnikov, in *Reviews of Plasma Physics,* Ed. by M. A. Leontovich (Consultants Bureau, New York, 1965), Vol. 1, p. 105.
16. V. V. Postupaev and D. V. Yurov, Plasma Phys. Rep. **42**, 1013 (2016). https://doi.org/10.1134/S1063780X16110076
17. A. D. Beklemishev, P. A. Bagryansky, M. S. Chaschin, and E. I. Soldatkina, Fusion Sci. Technol. **57**, 351 (2010). https://doi.org/10.13182/FST10-A9497

Translated by I. Grishina